Photophysical and Dynamic NMR Studies on 4-Amino-7-nitrobenz-2-oxa-1, 3-diazole Derivatives: Elucidation of the Nonradiative Deactivation Pathway

Satyen Saha and Anunay Samanta*

School of Chemistry, University of Hyderabad, Hyderabad 500 046, India

Received: May 7, 1998; In Final Form: July 10, 1998

A series of 4-aminonitrobenzoxadiazole (NBD) derivatives in which the amino nitrogen is part of a four- to seven-membered heterocyclic ring and a second series of 4-dialkylamino NBD derivatives with different alkyl chain lengths have been prepared and fully characterized and their photophysical properties investigated in an attempt to find out the nonradiative deactivation pathway of the fluorescent state in these systems. It is observed that the fluorescence properties of the NBD derivatives are highly sensitive to the structure of the amino moiety and the polarity of the surrounding media. It is shown that the nonradiative rate constants for the derivatives with large alkyl groups and large ring systems are considerably higher than those for systems with smaller alkyl groups and smaller ring systems. Dynamic NMR experiments have been carried out to probe the internal motion in the systems. The internal rotation around the bond connecting the amino nitrogen and the NBD ring is found to be rather slow in the ground state. The rate for the internal rotation is found to be the highest for the six-membered ring, and this has been interpreted in terms of the partial double bond character of the C−N bond. The results of the experiments seem to indicate that inversion of the amino nitrogen plays the most important role in determining the fluorescence efficiency of the systems.

1. Introduction

The electron donor−acceptor molecules have become the focus of extensive investigations in recent years primarily due to the fact that separation of charge is the basis of numerous transformations in chemistry and biology and an understanding of the photoinduced charge separation helps in understanding the mechanism of long-range separation of charge in plants during photosynthesis and designing efficient systems for solar energy conversion.[1] The donor−acceptor systems are also a favorite testing ground for the theories of electron transfer and solvation.[2] The organic conductors, superconductors, nonlinear optical materials, and a good majority of the fluorescence probes for the organized media are also systems of this class.[3]

A large number of systems in which the donor and acceptor moieties are connected by a single bond with the possibility of conjugation have been investigated in recent years with a view to understand the mechanism of *dual* fluorescence exhibited by them.[4−18] 4-Dimethylaminobenzonitrile (DMABN) is the most extensively studied system of this class.[4−18] It was believed that electronic excitation of DMABN leads to population of an electronic state in which one unit of charge is transferred from the dimethylamino group to the benzonitrile moiety and the donor and the acceptor orbitals are completely decoupled in a 90° twisted conformation.[6−8] While the '*normal*' fluorescence of DMABN originates from a locally excited (LE) state, the '*anomalous*' one originates from the highly dipolar twisted intramolecular charge transfer (TICT) state.[6−8] Even though the TICT mechanism was originally invoked by Grabowski and co-workers to account for the dual fluorescence of benzonitriles,[6−8] it was soon realized that the mechanism was helpful in understanding the fluorescence properties of a wide number of other donor−acceptor systems.[9−14] During the course of extensive investigations carried out over the past decade it was realized that the TICT state need not be fluorescent.[19−22] It is important to note in this context that whether fluorescent or not, a low-lying nonfluorescent TICT state can be responsible for the nonradiative decay of the fluorescent LE state in donor−acceptor systems exhibiting only '*normal*' fluorescence. Very recently, Zachariasse and co-workers have pointed out some of the deficiencies of the TICT model in explaining the photophysical behavior of the aminobenzonitrile derivatives.[15−18] Notable among them are (i) the absence of a linear correlation between the energy of the anomalous fluorescence band of the compounds and the redox potentials of the donor and the acceptor subgroups and (ii) observation of the anomalous fluorescence in systems where 90° twist of the amino group is not possible. A new model, termed as planar intramolecular charge transfer (PICT), has been proposed by Zachariasse et al. to interpret the photophysical behavior of aminobenzonitriles.[15−18] According to this model, inversion of the amino nitrogen is believed to be the promoting mode for the occurrence of the long-wavelength anomalous fluorescence band of DMABN. A second condition that is invoked in this model is that the energy gap between the two lowest excited states of aminobenzonitriles should be sufficiently small so as to allow vibronic coupling of the two states.

The present paper is concerned with a study of the fluorescence behavior of a series of donor−acceptor molecules (NBD derivatives) in which an amino group serves as the donor and a nitro group as the acceptor. NBD derivatives are known to be extremely popular candidates as fluorescent probes in biological applications.[23] NBD chloride[24] has often been used for labeling proteins with fluorescent groups and in studies of protein structure and conformational changes.[25,26] A large number of phospholipids and cholesterol analogues with NBD groups as fluorophores find application in the study of biological and model membranes.[27−29] The fluorescence quenching of the

* Corresponding author. E-mail: assc@uohyd.ernet.in. Fax: +91-40-3010120.

S1089-5639(98)02154-9 CCC: $15.00 © 1998 American Chemical Society
Published on Web 09/23/1998

CHART 1

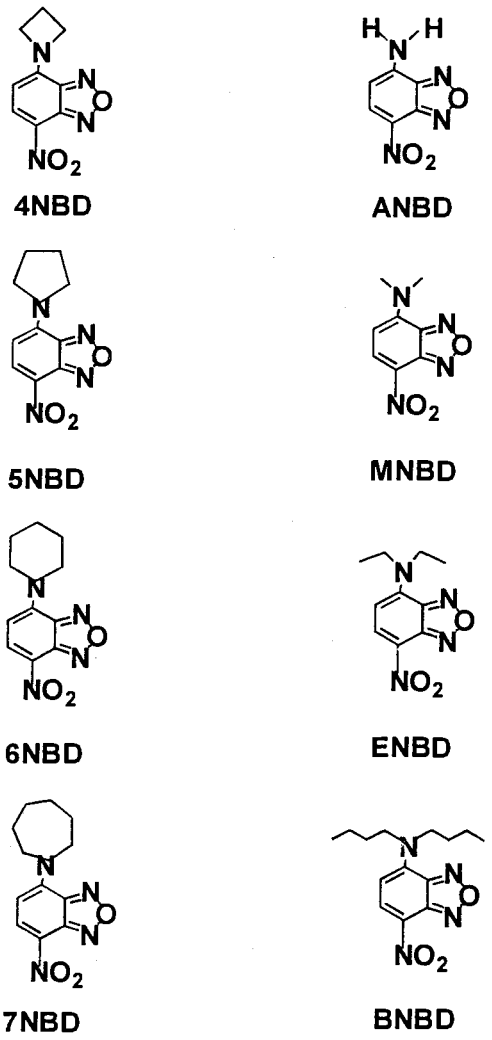

NBD moiety by transition-metal ions has also been used in determining the location of the fluorophore in complex media.[30] The fluorescence response of a few NBD derivatives toward different guests has been studied.[31−34] We have recently studied the fluorescence sensory behavior of some NBD fluorophore-labeled supramolecular systems toward the quenching transition-metal ions.[35] The solvent polarity dependence of a few NBD derivatives has recently been reported, where the involvement of a nonfluorescent TICT state in the nonradiative decay of the fluorescent state has been speculated.[36] We have undertaken this work on two series of the NBD derivatives (Chart 1) with a view to find out the nature of the nonradiative pathway in this class of systems. In particular, we have examined in this paper whether the TICT model proposed by Grabowski[6−8] or the recent PICT model proposed by Zachariasse[15−18] is best suited for the description of the photophysical behavior of the NBD derivatives. The photophysical measurements have been supplemented by dynamic NMR spectroscopic measurements. To the best of our knowledge, this is the first study where measurements of this kind have been performed specifically to understand the photophysical responses of the donor−acceptor systems.

2. Experimental Section

2.1. Materials. 4-Chloro-7-nitrobenzofurazan (NBD-chloride), trimethyleneimine(azetidine), and hexamethyleneimine

SCHEME 1

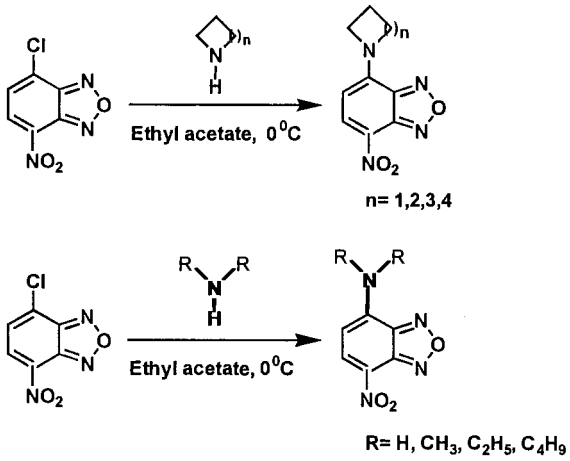

were received from Fluka and were used as received. Pyrrolidine and piperidine from Aldrich, dimethylamine (40 wt % solution in water), diethylamine, and *n*-dibutylamine were received from Acros and were distilled before use. Since extremely pure and dry solvents are essential for spectroscopic measurements involving dipolar species, all the solvents used in this investigation for spectroscopic measurements were rigorously purified following standard procedures.[37] The extent of dryness of each solvent was checked by monitoring the wavelength of the absorption maximum of a polarity-sensitive betaine dye in the given solvent and comparing the same with the literature value of the solvent.[38]

Most of the compounds synthesized are new and are listed in Chart 1 with the structures and the abbreviated names. All the compounds were prepared following a general procedure outlined in Scheme 1. In this method, NBD-chloride (1 mmol) was dissolved in 3 mL of ethyl acetate. The amine (1.2 mmol) was diluted in 2 mL of ethyl acetate and was added slowly dropwise to an NBD-chloride solution with stirring in an ice bath. After stirring for 30 min in the ice bath, the reaction mixture was then stirred for another 2 h at room temperature. The product, which appeared as a red precipitate, was filtered out and purified by column chromatography using silica gel column. Hexane and ethyl acetate were used as eluent in different proportion for the purification of different compounds. The purified compounds were recrystallized from absolute ethanol. The products were confirmed by IR and NMR spectroscopy. A few compounds for which single crystals were obtained were also characterized by X-ray crystallography.

2.2. Apparatus and Methods. The fluorescence quantum yields of the NBD derivatives were measured using fluorescein as the reference compound ($\phi_f = 0.90$ in 0.1 N NaOH).[39] A solution of the NBD derivative in any given solvent was prepared with an absorbance (OD $\approx$0.15) the same as that of the reference compound at the excitation wavelength. The fluorescence spectra were measured under the same operating conditions, and the settings and quantum yields were determined by comparing the areas underneath the fluorescence spectra by the 'cut and weigh' method.

The absorption and the fluorescence spectra were recorded on a Jasco UV−vis spectrophotometer (model 7800) and a Hitachi spectrofluorimeter (model 4010), respectively. The fluorescence decay curves were recorded using an IBH single-photon-counting spectrofluorimeter (model 5000U). The instrument was operated with a thyratron-gated flash lamp filled with hydrogen at a pressure of 0.5 atm. The lamp was operated at a frequency of 40 kHz, and the pulse width of the lamp under

the operating condition was ~1.2 ns. The lifetimes were estimated from the measured fluorescence decay curves and the lamp profile using a nonlinear least-squares iterative fitting procedure.[40] The goodness of the fit was evaluated from the χ^2 values and the plot of the residuals.

The IR and ^{1}H NMR spectra were recorded on a JASCO FT-IR (model 5300) and a Bruker ACF-200 spectrometer (200 MHz), respectively. The NMR measurements have been carried out in $CDCl_3$.

The crystal structures of a few compounds were determined using an Enraf-Nonius single-crystal diffractometer (MACH 3), employing CAD-4 Software (version 5.0). Structure solution and refinement were done by SHELXS-97 and SHELXL-97 software, respectively.

The theoretical calculations based on the semiempirical AM1 (Austin Model 1) method[41,42] were carried out using the Hyperchem package (release 5.0) obtained from Hypercube, Inc. The calculations were performed on a personal computer. The initial optimization of the structures was achieved using the MM+ method. Subsequently, unrestricted geometry optimizations at the semiempirical level were performed to obtain the ground-state dipole moments and the structural parameters of the molecules. The optimization of the ground-state geometry of the molecules was achieved using a conjugate gradient (Polak−Ribiere) type of algorithm with a root-mean-square (rms) gradient as the convergence criterion. The rms gradient was kept below 0.001 kcal/(Å mol). The excited-state dipole moments were obtained for the ground-state-optimized structures of the molecules using configuration interaction (singly excited, orbital criteria: HOMO = 8, LUMO = 8).

3. Results and Discussion

3.1. Photophysical Behavior. *3.1.1. Absorption Spectra.* The absorption spectra of the NBD derivatives are characterized by broad bands. The lowest energy absorption maximum displays solvatochromic behavior typical of a charge-transfer transition in which the amino group acts as a donor and the nitro group as an acceptor. The intramolecular charge transfer in the NBD chromophore is in agreement with that observed in structurally similar but relatively more extensively investigated *p*-nitroaniline.[43−49] A few representative absorption spectra of 5NBD are illustrated in Figure 1. As seen from the figure, with an increase in the polarity of the medium, the lowest energy absorption band maximum exhibits a gradual bathochromic shift. A typical shift of the absorption maximum on change of the solvent ranges between 16 and 22 nm in aprotic media. In protic media, the bathochromic shift of the absorption maximum is considerably larger, presumably due to the specific hydrogen-bonding interaction between the NBD derivatives and the solvent molecules. The absorption and emission spectral data of the NBD derivatives in a series of solvents are collected in Table 1. It can be seen from the table that for ANBD, the position of the absorption maximum in any given solvent is drastically different from that of the other derivatives. Among the ring systems, the wavelength of the absorption maxima does not show any appreciable variation with change in the heterocyclic ring size, and for the alkyl derivatives, the band maximum shifts gradually toward red with increasing chain length of the alkyl groups. These observations can be rationalized in terms of the inductive influence of the various groups.

3.1.2. Fluorescence Spectra. The NBD derivatives are known to display broad emission bands devoid of any fine structure due to the intramolecular charge-transfer (ICT) nature of the fluorescence.[36] The ICT is also evident from the solvatochromic response of the fluorescence band. In aprotic media, the fluorescence maximum displays a Stokes shift with an increase in the polarity of the solvent (Figure 2). A comparatively larger bathochromic shift for the fluorescence band maximum (Table 1) in comparison with that for the absorption is indicative of an excited state that is relatively more polar than the ground state. As far as the influence of the structure of the molecules on the wavelength of the fluorescence maximum is concerned, in any given solvent, no significant variation could be noticed among the alkylated or ring systems. However, ANBD displays its maximum at a wavelength much lower than those observed for the other derivatives. This is clearly due to the absence of the inductive influence of the alkyl groups in the system.

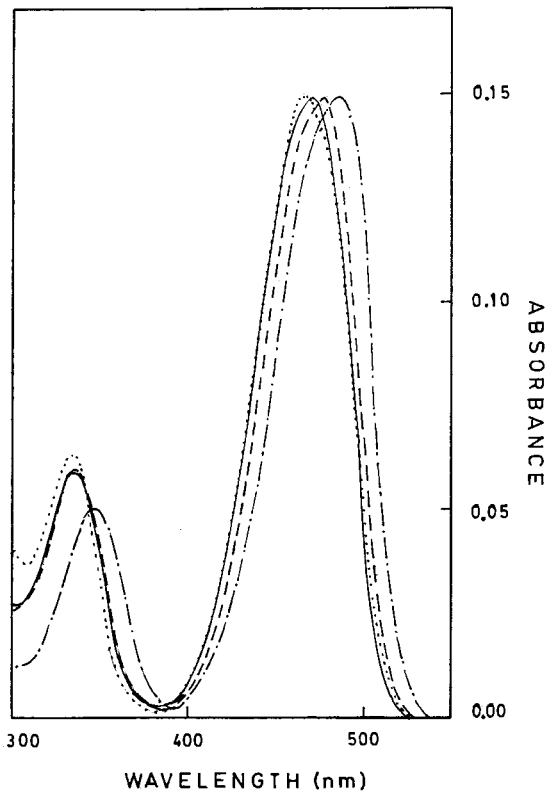

Figure 1. Absorption spectra of 5NBD in toluene (···), 1,4-dioxane (—), tetrahydrofuran (- - -) and acetonitrile (- · -) at room temperature.

3.1.3. Dipole Moment Change on Electronic Excitation. Attempts were made to quantify the extent of charge separation on electronic excitation of the various NBD derivatives, in particular, to evaluate the change in the dipole moment ($\Delta\mu$) from an analysis of the Stokes shift between the wavenumbers of the absorption and the fluorescence maxima ($\Delta\nu = \bar{\nu}_a - \bar{\nu}_f$) as a function of the solvent polarity parameter, Δf

$$\left(= \frac{\epsilon - 1}{2\epsilon + 1} - \frac{n^2 - 1}{2n^2 + 1}\right)$$

based on the Lippert−Mataga equation,[50−52]

$$\bar{\nu}_a - \bar{\nu}_f = \frac{2(\mu_e - \mu_g)^2}{hca^3}\left[\frac{\epsilon - 1}{2\epsilon + 1} - \frac{n^2 - 1}{2n^2 + 1}\right] + \text{constant} \quad (1)$$

where, $\bar{\nu}_a$ and $\bar{\nu}_f$ are the wavemnumbers of the absorption and fluorescence maxima, μ_g and μ_e are the ground- and excited-state dipole moments, ϵ and n are the dielectric constant and

TABLE 1: Absorption and Emission Spectral Data of the NBD Derivatives in Different Solvents at Room Temperature[d]

compounds	toluene λ_{ma}^{abs} (nm)	toluene λ_{ma}^{flu} (nm)	dioxane λ_{ma}^{abs} (nm)	dioxane λ_{ma}^{flu} (nm)	THF[a] λ_{ma}^{abs} (nm)	THF[a] λ_{ma}^{flu} (nm)	DCM[b] λ_{ma}^{abs} (nm)	DCM[b] λ_{ma}^{flu} (nm)	acetone λ_{ma}^{abs} (nm)	acetone λ_{ma}^{flu} (nm)	ACN[c] λ_{ma}^{abs} (nm)	ACN[c] λ_{ma}^{flu} (nm)	ethanol λ_{ma}^{abs} (nm)	ethanol λ_{ma}^{flu} (nm)	methanol λ_{ma}^{abs} (nm)	methanol λ_{ma}^{flu} (nm)	water λ_{ma}^{abs} (nm)	water λ_{ma}^{flu} (nm)
4NBD	467	524	468	530	472	530	477	530	481	536	483	542	480	545	481	545	499	572
5NBD	467	517	468	523	472	524	478	525	478	532	484	537	481	539	481	543	500	560
6NBD	468	528	470	533	474	536	482	539	483	543	487	551	487	551	484	551	508	571
7NBD	468	522	470	525	477	526	479	529	481	538	485	543	483	543	484	551	505	562
ANBD	423	504	436	515	445	517	429	504	442	515	445	521						
MNBD	461	519	465	527	468	527	473	526	473	534	478	539	481	540	477	541	497	558
ENBD	468	521	471	528	473	529	479	530	480	536	484	540	476	539	483	545	503	561
BNBD	471	522	471	530	477	530	485	531	483	538	487	543	486	542	486	545	506	557

[a] Tetrahydrofuran is represented as THF. [b] Dichloromethane is shown as DCM. [c] Acetonitrile is indicated as ACN. [d] The fluorescence spectra were measured by exciting at the absorption maxima of the compounds.

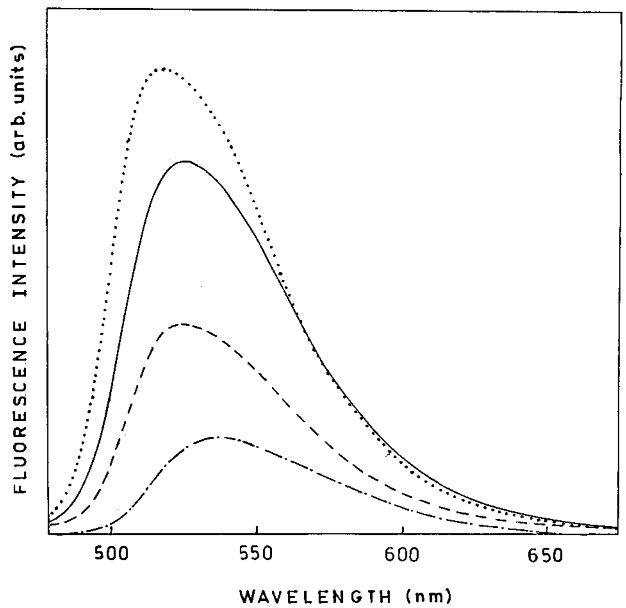

Figure 2. Fluorescence spectra of 5NBD in toluene (···), 1,4-dioxane (—), tetrahydrofuran (- - -) and acetonitrile (- · -) at room temperature. The solutions were excited at 470 nm.

TABLE 2: AM1-Calculated Ground-State (μ_g) and Excited-State (μ_e) Dipole Moments of the NBD Derivatives

compound	μ_g (D)	μ_e (D)	$\Delta\mu$ (D)
4NBD	9.64	11.97	2.33
5NBD	10.54	12.67	2.13
6NBD	9.30	12.61	3.31
7NBD	9.98	12.60	2.62
MNBD	9.96	12.11	2.15
ENBD	9.86	12.24	2.38
BNBD	10.31	12.54	2.23

refractive index of the medium, *c* is the velocity of light, and *a* is the Onsager cavity radius.

However, since the correlation between and $\Delta\bar{\nu}$, and Δf was found to be rather poor (correlation coefficient, $r = 0.2-0.3$), no estimate of $\Delta\mu$ could be obtained from this analysis. In this context, it may be noted that a similar observation was made earlier by Forgues et al. in the case of diethylamino derivative of NBD.[36] Since it is generally observed that $\Delta\bar{\nu}$ values are correlated to the microscopic solvent polarity parameter (E_T-(30) or E_T^N) better than to the polarity function (Δf),[53-55] involving bulk properties such as the dielectric constant and refractive index, we made another attempt to evaluate the $\Delta\mu$ values for the systems based on a recently suggested procedure.[53] According to this procedure,[53] the $\Delta\bar{\nu}$ is related to E_T^N as follows:

$$\bar{\nu}_a - \bar{\nu}_f = 11307.6\{(\Delta\mu/\Delta\mu_D)^2(a_D/a)^3\}E_T^N + \text{constant} \quad (2)$$

Where, $\Delta\mu_D$ and a_D represent the dipole moment change and Onsager cavity radius, respectively, for the betaine dye. However, for the NBD derivatives, the plots based on this equation, although superior to those obtained using eq 1, were still far from satisfactory (*r* between 0.7 and 0.8) to allow estimation of reliable $\Delta\mu$ values. Having not succeeded in obtaining the $\Delta\mu$ values of the compounds from the solvatochromic data, we have calculated these values for the AM1-optimized structures of the compounds. The $\Delta\mu$ values for the ground and first excited singlet state were found to lie between 2.1 and 3.3 D (Table 2). These values are in agreement with the literature values of structurally similar compounds.[56]

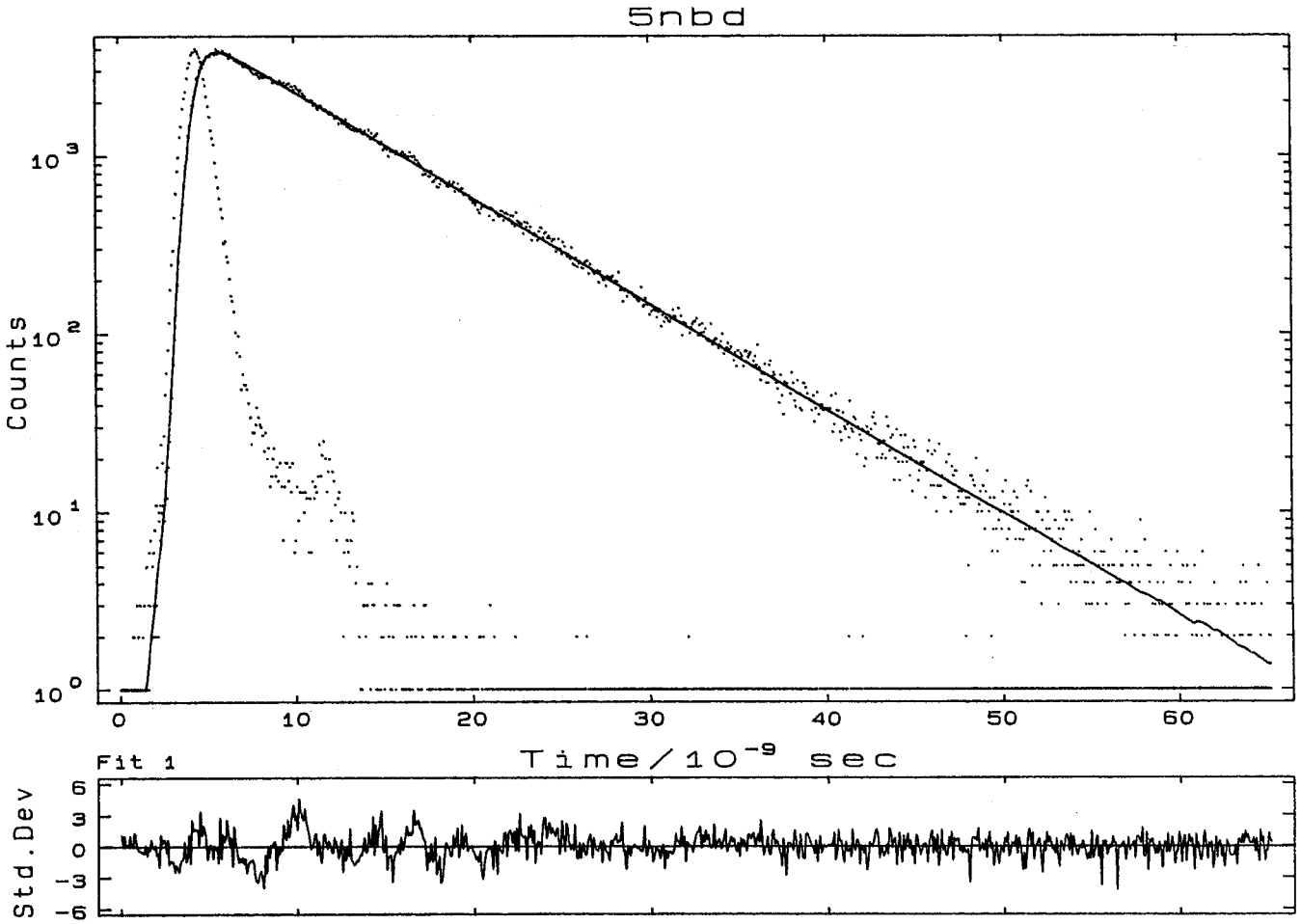

Figure 3. Fluorescence decay curve of 5NBD in 1,4-dioxane at room temperature. The decay was measured at 520 nm. Shown also are the excitation lamp profile and the best fit to the fluorescence decay (single-exponential fit with a lifetime of 7.32 ns).

TABLE 3: Fluorescence Quantum Yields (ϕ_f) of the Cyclic and Linear NBD Derivatives in Different Solvents at Room Temperature

solvent	E_T (30)	4NBD	5NBD	6NBD	7NBD	ANBD	MNBD	ENBD	BNBD
toluene	33.9	0.49	0.49	0.48	0.28	0.13	0.52	0.48	0.48
dioxane	36.0	0.57	0.41	0.12	0.07	0.46	0.15	0.08	0.08
THF	37.4	0.59	0.22	0.03	0.02	0.79	0.14	0.03	0.02
DCM	40.7	0.51	0.27	0.03	0.02	0.45	0.16	0.03	0.02
acetone	42.2	0.52	0.12	0.01	0.01	0.51	0.02	0.01	0.01
ACN	45.6	0.44	0.11	0.01	0.01	0.57	0.02	0.01	0.01
ethanol	51.9	0.22	0.06	0.01	0.01		0.01	0.02	0.01
methanol	55.4	0.19	0.06	0.01	0.01		0.02	0.01	0.01
water	63.1	0.02	0.01	0.002	0.004		0.01	0.01	0.01

3.1.4. Fluorescence Quantum Yield and Lifetime. The fluorescence quantum yields (ϕ_f) of the various NBD derivatives in a series of solvents of different polarities are collected in Table 3. These data can be summarized as follows. First, the ϕ_f values of the systems are significantly higher in aprotic media compared to those in the protic media because of specific hydrogen-bonding interactions in the latter solvents. Second, ϕ_f of ANBD, the system with a free amino group, is the highest among all the compounds in any given solvent except in toluene. Third, in a given solvent, with an increase in the length of the alkyl group or the ring size, the quantum yield decreases steadily. Fourth, for a given system, as the polarity of the medium is increased, the fluorescence quantum yield is decreased, and this solvent polarity induced decrease in the fluorescence yield is most pronounced for systems with higher ring size or larger alkyl groups.

The fluorescence lifetimes (τ_f) of the NBD derivatives have been estimated in several solvents from the measured fluorescence decay curves. A typical fluorescence decay curve along with the single-exponential fit to the data is shown in Figure 3. The τ_f values of the systems in different solvents are collected in Table 4. The τ_f values of ANBD and 4NBD are found to be least sensitive to the polarity of the medium. On the other hand, for higher ring systems and alkyl derivatives, even though τ_f is fairly high in nonpolar toluene, it drastically decreases as the polarity of the surrounding environment is increased. Both the ϕ_f and τ_f values indicate clearly that a nonradiative relaxation pathway is operational for the alkyl derivatives and higher membered ring systems, particularly in relatively polar media.

One point that perhaps deserves some mention is that both the ϕ_f and τ_f values of ANBD are surprisingly low in the least

TABLE 4: Fluorescence Lifetimes (ns) of the NBD Derivatives in Different Solvents[a]

compound	toluene	dioxane	THF	DCM	acetone	ACN	ethanol	methanol	water
4NBD	9.81	10.70	10.85	9.84	10.80	9.96	5.73	5.32	1.00
5NBD	9.08	7.32	4.29	5.09	2.41	2.24	1.57	1.78	0.42
6NBD	7.74	1.98	0.58	0.57	0.32	0.16	0.14	0.15	
7NBD	4.54	0.98	0.42	0.32	0.27	0.12	0.22	0.20	0.10
ANBD	3.59	10.62	11.70	6.49	9.12	11.45			
MNBD	9.74	3.06	2.87	2.72	0.43	0.44	0.30	0.45	0.13
ENBD	7.64	1.53	0.51	0.52	0.27	0.27	0.44	0.29	0.07
BNBD	7.50	1.48	0.48	0.41	0.21	0.18	0.27	0.23	0.21

[a] The solutions were excited at the respective absorption maxima of the compounds. The fluorescence decays were found to be single exponential in most of the cases. In some cases, particularly in hydrogen-bonding solvents, the decays consisted of a minor second component, which was neglected. The measurement error is ±10% for lifetimes above 1 ns. The lifetimes below 1 ns indicate only the trend.

TABLE 5: Nonradiative Rate Constants (10^8 s^{-1}) of the NBD Derivatives in Aprotic Solvents at Room Temperature

solvent	4NBD	5NBD	6NBD	7NBD	ANBD	MNBD	ENBD	BNBD
toluene	0.52	0.56	0.62	1.59	2.44	0.49	0.68	0.70
dioxane	0.40	0.80	4.42	9.48	0.50	2.77	6.04	6.20
THF	0.38	1.82	16.74	23.38	0.18	2.99	18.89	20.48
DCM	0.50	1.43	17.03	30.66	0.84	3.07	18.39	23.89
acetone	0.45	3.63	30.87	36.62	0.53	22.56	36.46	46.60
ACN	0.57	3.96	62.14	82.58	0.37	22.12	36.49	54.15

polar solvent, toluene. One can rationalize this behavior by considering the existence of two close-lying states (CT and nπ^*) in the systems. In the least polar solvent, toluene, low ϕ_f and τ_f values for ANBD are presumably due to the fact that the emission originates from the nπ^* state, which is the lowest excited state. In relatively higher polarity solvents, the CT state is stabilized below the nπ^* states, accounting for the enhancement of the ϕ_f and τ_f values. For all other systems, because of the inductive influence, the CT state is lower than nπ^* state even in toluene.

3.1.5. The Nonradiative Rate Constants. We have evaluated the nonradiative rate constants (k_{nr}) of all the derivatives in several aprotic media from the measured fluorescence yield (ϕ_f) and lifetime (τ_f) using $k_{nr} = (1 - \phi_f)/\tau_f$, and the same are collected in Table 5. As seen from the table, while the k_{nr} values of ANBD and 4NBD do not vary appreciably in different media, those of the remaining derivatives are severalfold higher in polar media compared to the nonpolar media. As mentioned in section 1, the dependence of k_{nr} values on the solvent polarity was noted in the case of ENBD, and it was speculated that twisting of the dialkylamino group about the C−N bond that connects this group with the NBD chromophore (henceforth simply referred to as C−N bond) is the nonradiative deactivation pathway.[36] As will be shown in the following sections, when the photophysical data of all the derivatives are taken into consideration, it becomes difficult to interpret them in terms of the TICT mechanism.

3.2. Dynamic NMR Spectroscopy. The room-temperature proton magnetic resonance spectra of the NBD derivatives, which were primarily obtained to establish the structural identity of the compounds, were found to be unusually broad for some systems, which suggests an exchange of the nuclear sites. Since the nuclear motion, whether internal rotation or any other, is likely to affect the decay of the emitting state, the exchange process has been investigated by dynamic NMR spectroscopy.[57] Figure 4 illustrates the room-temperature NMR spectra of the cyclic derivatives. It can be seen that the NMR signal that appears at around 3−5 δ is unusually broad for 7NBD. In the case of 4NBD and 5NBD, the signal appears as two broad doublets, whereas one sharp peak is observed for 6NBD at room temperature. Since this behavior is a reflection of a dynamic process in which the nuclear sites are exchanged in the molecule, the NMR spectra of all the systems have been studied as a function of the temperature. Figure 5 illustrates the variation of the NMR signals of interest for the cyclic compounds as a function of the temperature. Two clearly resolved triplets could be observed on lowering of the temperature in all cases.

Several different internal motions in the systems, such as twisting around the C−N bond (internal rotation), inversion of the amino nitrogen, and ring inversion (Scheme 2), may give rise to broad NMR peaks. The fact that ring inversion is not responsible for the broadening of the NMR signal is evident from the fact that (i) the linear alkyl derivatives of NBD also give rise to similar broad peaks that can be resolved at lower temperatures and (ii) the ring inversion process is known to be too rapid for the four- and five-membered ring systems to be observed on the NMR time scale.[57] It should be noted in this context that since the axial and equatorial proton signals are not resolvable in the present experimental condition, nitrogen inversion that leads to an exchange of the nuclei bearing the hydrogen atoms (Scheme 2) cannot be responsible for the broad NMR signal. Therefore, the nuclear exchange process observed here has to be assigned to the internal rotation (or twisting, as it is more commonly called) about the C−N bond. The peaks observed between 3 and 5 δ (integration corresponding to four protons) should be assigned to the two sets of methylene protons adjacent to the amino nitrogen atom. The chemical shifts of these two sets of protons are different because of the difference in their environments due to the presence of the diazaoxazole ring on one side. At lower temperature, when the internal rotation is slow, the methylene groups display two signals (each appearing as triplet) typical of an AB system. On the other hand, at higher temperature, when the internal rotation is fast, a sharp signal is observed. Between the slow and the fast exchange limits, changes in the line shape of the NMR signals are observed. The separation between the two sets of peaks and the temperature at which they coalesce (T_c) have been measured for all the systems, and the values are tabulated in Table 6. The rate constant of the internal rotation (k_c) at the coalescence temperature has been obtained using the following equation:[57]

$$k_c = \pi\Delta\nu/\sqrt{2} \tag{3}$$

where $\Delta\nu$ is the difference in the chemical shifts of the two

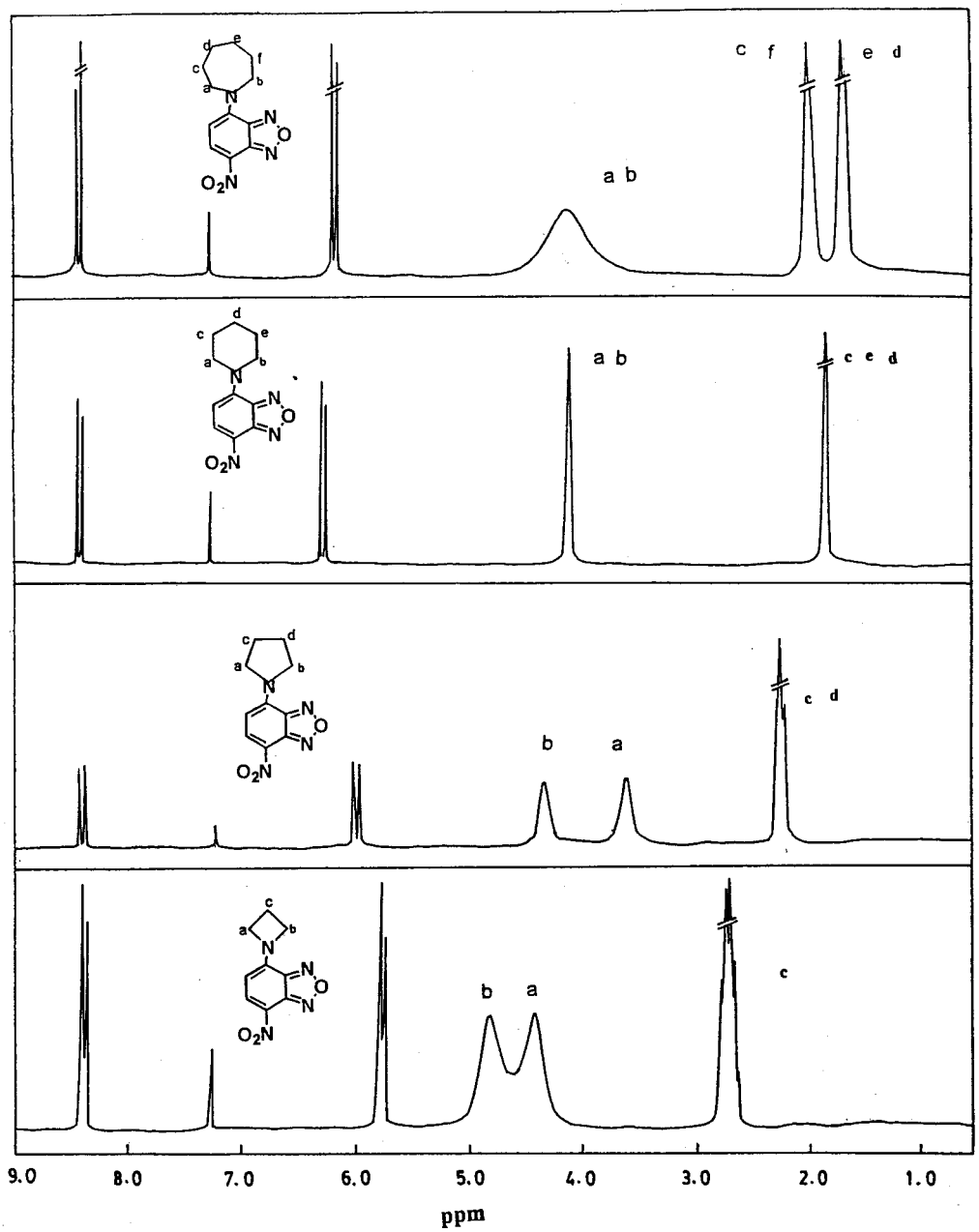

Figure 4. NMR spectra of the cyclic NBD derivatives in $CDCl_3$ at 25 °C.

sites. The free energy of activation ($\Delta G^{\ddagger}_c$) for the exchange has been obtained using[57] the following equation:

$$\Delta G^{\ddagger}_c = 4.57 T_c \left(9.97 + \log \frac{T_c}{\Delta \nu}\right) \qquad (4)$$

It can be seen from the $\Delta G^{\ddagger}_c$ values, collected in Table 6, that for the alkyl derivatives, the barrier to internal rotation increases marginally with an increase in the size of the alkyl group. On the other hand, for the ring systems, even though the barrier height was expected to increase with an increase in the size of the ring, the results indicate the $\Delta G^{\ddagger}_c$ value to be the lowest for the six-membered ring system. We have found out that this apparently unusual behavior is linked to the partial double bond character of the C−N bond. It may be noted that had there been no double bond character of the C−N bond, the barrier to internal rotation would have been considerably lower and perhaps the barrier would have increased with an increase in the size of the ring. However, since the C−N bond is expected to have considerable double bond character because of intramolecular charge separation between the amino and the nitro group in the fluorophore, the rotational barrier is expected to be governed mainly by the extent of the double bond character of the C−N bond rather than by the size of the group. Since both the C−N bond length and the ground-state dipole moments of the compounds are reasonably good measures of the double bond character of the concerned bond, one expects, on the basis of the NMR results, the six-membered ring system to have the lowest ground-state dipole moment and highest C−N bond length among the ring systems. The data presented in Table 7 show that that is indeed the case. The results of the X-ray crystallographic measurements on a few systems also indicate the C−N bond length to be shorter than the single bond distance.[58] A plot of the measured $\Delta G^{\ddagger}_c$ values versus the ground-state dipole moments of the ring systems (Figure 6) clearly shows that the barrier to the twisting or internal rotation

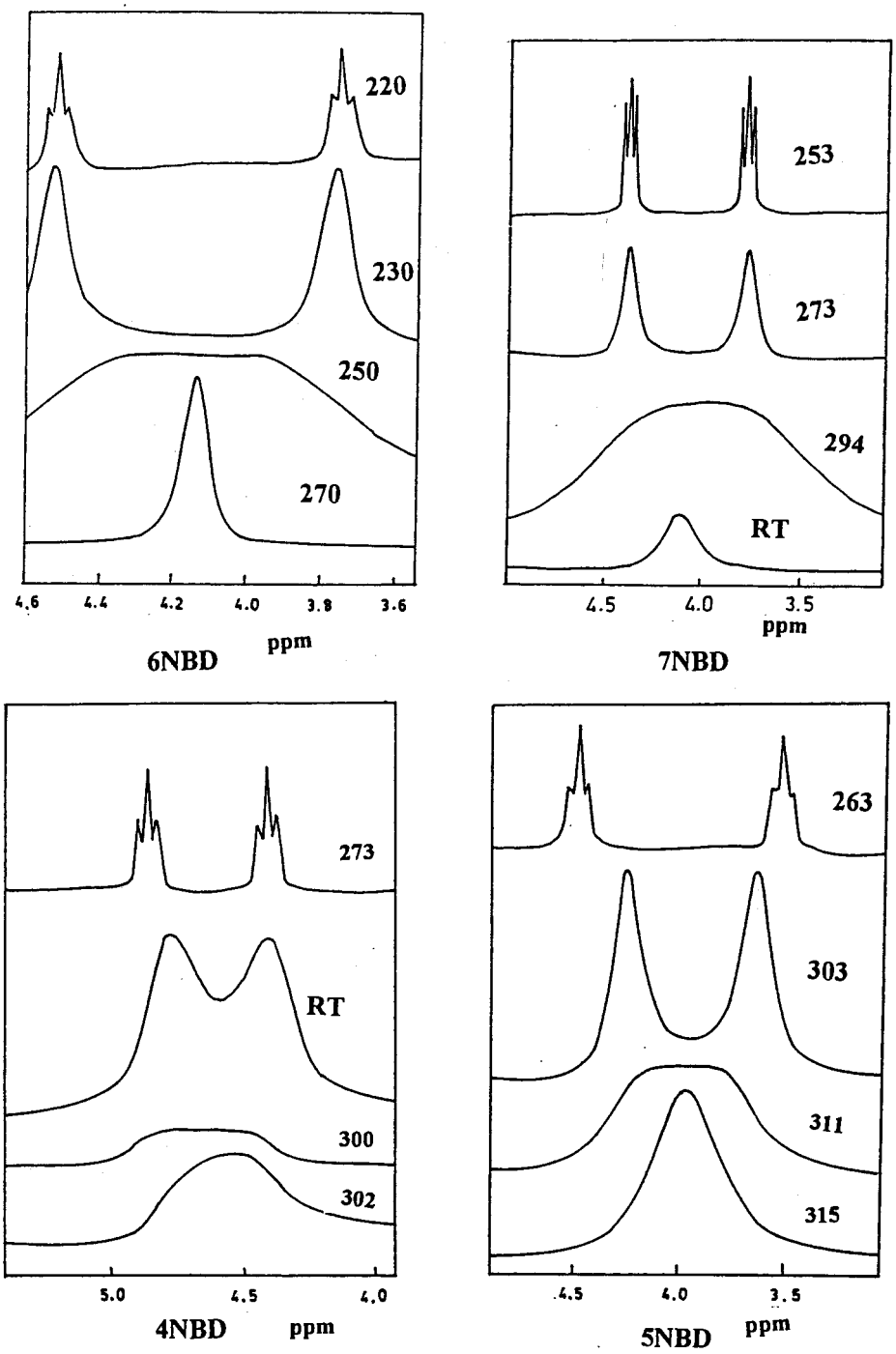

Figure 5. NMR spectra of the cyclic NBD derivatives in $CDCl_3$ as a function of temperature (K). Only the NMR peaks of interest are shown here.

around the C−N bond is governed by the bond order of the system rather than by the ring size.

4. Discussion and Conclusion

The NBD derivatives, as found in this investigation and elsewhere,[36] display only one emission band. The fluorescence originates from an LE state with charge-transfer character (except for ANBD in highly nonpolar solvents), and the dipole moment of this state is slightly higher than that of the ground state. The fluorescence yield, lifetime, and the nonradiative rate constants of the NBD derivatives are strongly dependent on the structure of the amino moieties. While for ANBD and 4NBD, the k_{nr} values are low and do not depend significantly on the polarity of the surrounding media, the k_{nr} values for the other derivatives are considerably higher, particularly in the polar media. Since the ground-state structure of the donor−acceptor molecules often dictate the photophysical properties of these derivatives, we have probed the ground-state structure of the systems by AM1 calculations and investigated the internal motion in the systems using dynamic NMR spectroscopic technique.). These studies reveal that the amino nitrogen atom in the systems is slightly pyramidal in the ground state,[59] with the C−N bond having some partial double bond character. The internal rotation about the C−N bond is measured to be rather slow because of the double bond character. The other internal motions such as nitrogen inversion in all the systems and ring inversion in the cyclic systems could not be observed as these motions either are too rapid compared to the NMR time scale

SCHEME 2

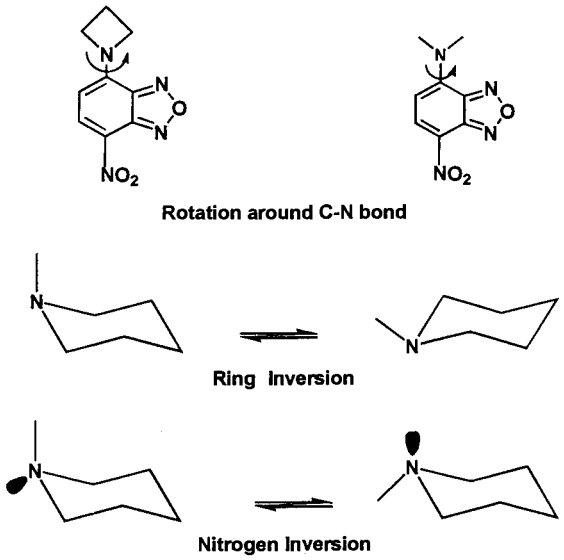

TABLE 6: Coalescence Temperature (T_c), Difference in Chemical Shifts of the Two Sites ($\Delta\nu$), Rate Constant of the Exchange (k_c) at the Coalescence Temperature, and the Barrier to Rotation ($\Delta G^{\ddagger}_c$) about the C−N Bond in the NBD Derivatives

compounds	T_c (K)	$\Delta\nu$ (Hz)	k_c (s^{-1})	$\Delta G^{\ddagger}_c$ (kJ/M)
4NBD	302	88.2	197.5	59.9
5NBD	312	127.1	275.5	62.0
6NBD	250	151.6	336.7	48.1
7NBD	293	120.0	266.6	57.1
MNBD	275	105.8	235.0	54.8
ENBD	274	100.9	224.1	54.7
BNBD	282	105.7	234.8	55.4

or do not lead to an exchange of the hydrogen nuclei. Since the fluorescent state of the NBD derivatives is shown to be more polar than the ground state, one can expect the double bond character of the C−N bond to be higher and the amino nitrogen to be more planar in the excited state as compared to the ground state. Consideration of these factors led us to suggest that the barrier to the internal rotation around the C−N bond is higher in the excited state. Consequently, the internal rotation is expected to be slower in the excited state and hence can not be expected to be an important factor in determining relatively much faster nonradiative decay of the systems. We can discount the possibility of internal rotation affecting the nonradiative rates in the systems using a different line of argument. One can conclude based on the measured data on the rotational rates of the systems that if internal rotation in the excited state is responsible for the observed variation of the nonradiative rates in different systems, then in any given solvent, the nonradiative rate should have been the highest for 6NBD among the ring systems and for MNBD and ENBD among the alkyl derivatives. However, it is clear from the data shown in Table 5 that k_{nr} values are not in accordance with the trend one expects based on consideration of internal rotation or twisting as the promoting mode for the nonradiative decay process.

Among the other possible modes of internal motion, inversion of the ring, which is known to be fast enough to compete with the radiative process, could not be considered as a dominant mechanism in these systems for the following reasons. First, this motion does not lead to any change in the configuration of the amino nitrogen and hence is not expected to affect the fluorescence efficiency of the systems. Second, this motion is known to be extremely rapid in the case of four- and five-membered rings[57] and hence according to this mechanism, the fluorescence efficiencies of 4NBD and 5NBD should have been the lowest (which is not the case). Finally, the open dialkylamino systems, where this motion is not possible, also display nonradiative decay similar to that exhibited by the ring system.

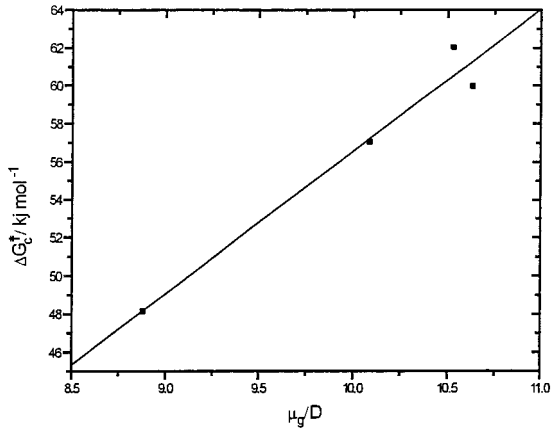

Figure 6. Plot of $\Delta G^{\ddagger}_c$ values versus the ground-state dipole moments (μ_g) of the cyclic NBD derivatives. The straight line represents the best linear fit to the data ($r = 0.98$).

TABLE 7: AM1-Calculated Bond Length and Ground-State Dipole Moment (μ_g) of the Ring Systems

compound	μ_g (D)	C−N bond length (Å)
4NBD	9.64	1.3678
5NBD	10.54	1.3601
6NBD	9.30	1.3841
7NBD	9.98	1.3783

On the basis of the above considerations, we are led to conclude that nitrogen inversion, which is also known to be a fast process, is responsible for the nonradiative decay of the excited state of the NBD derivatives. Even though this motion has not been observed by NMR, it is known in the literature that the barrier to nitrogen inversion in trialkylamines is much lower in the range of 6−8 kcal mol^{-1}, and this barrier is lowered as the size of the alkyl group is increased.[60] For the ring systems, it is reported that nitrogen inversion is the slowest in the case of three-membered nitrogen-containing heterocycles (aziridines).[57] As the ring size is increased, the barrier to nitrogen inversion is known to decrease steadily. This behavior has been rationalized in terms of the strain in the planar conformation of the molecule, which is close to the transition state for the inversion process. It is therefore evident that the k_{nr} values of the NBD derivatives agree rather well with the rates of the nitrogen inversion motion.

In summary, the photophysical behavior of several new NBD derivatives as a function of their structure and the polarity of the media has been studied. To rationalize the fluorescence response of the systems, dynamic NMR spectroscopic measurements, AM1 calculations, and X-ray crystallographic measurements have been performed. The results of these measurements indicate the inadequacy of the TICT model in explaining the photophysical behavior of the systems. The inversion of the amino nitrogen seems to be responsible for the nonradiative decay in the systems.

Acknowledgment. The research described herein is supported by grants received from Department of Science and Technology, Government of India. S.S. thanks the University Grants Commission for a fellowship.

References and Notes

(1) (a) Michel-Beyerle, M. E. *The Reaction Centre of Photosynthetic Bacteria*; Springer-Verlag: Berlin, 1995. (b) Diner, B. A.; Babcock, G. T. In *Structure, Dynamics, and Energy Conversion Efficiency in Photosystem II*; Diner, B. A., Babcock, G. T., Ed.; Kluwer: Dordrecht, 1996; p 213. (c) Wasielewski, M. R. *Chem. Rev.* **1992**, *92*, 435. (d) Gust, D.; Moore, T. A.; Moore, A. L. *Acc. Chem. Res.* **1993**, *26*, 198. (e) Kurreck, H.; Huber, M. *Angew. Chem., Int. Ed. Engl.* **1995**, *34*, 849. (f) Bard, A.; Fox, M. A. *Acc. Chem. Res.* **1995**, *28*, 141. (g) Memming, R. In *Photochemical Conversion and Storage of Solar Energy*; Pelizetti, E., Schiavello, M., Ed.; Kluwer: Holland, 1991; p 193. (h) Meyer, T. J. *Acc. Chem. Res.* **1989**, *22*, 163.

(2) Barbara, P. F.; Jarzeba, W. *Acc. Chem. Res.* **1988**, *21*, 195.

(3) (a) Kanis, D. R.; Ratner, M. A.; Marks, T. J. *Chem. Rev.* **1994**, *94*, 195. (b) Shelton, D. B.; Rice, J. E. *Chem. Rev.* **1994**, *94*, 3. (c) Chemla, D. S.; Zyss, J. *Nonlinear Optical Materials of Organic Molecules and Crystals*; Academic Press: New York, 1987. (d) Kalyanasundaram, K. *Photochemistry in Microheterogeneous Systems*; Academic Press: New York, 1987.

(4) Lippert, E.; Lüder, W.; Moll, F.; Nagele, H.; Boos, H.; Prigge, H.; Blankenstein, I. S. *Angew. Chem.* **1961**, *73*, 695.

(5) Lippert, E.; Luder, W.; Boos, H. In *Advances in Molecular Spectroscopy*; Mangini, A., Ed.; Pergamon Press: New York, 1962.

(6) Grabowski, Z. R.; Dobkowski, J. *Pure Appl. Chem.* **1983**, *55*, 245.

(7) Rotkiewicz, K.; Grellman, K. H.; Grabowski, Z. R. *Chem. Phys. Lett.* **1973**, *19*, 315.

(8) Grabowski, Z. R.; Rotkiewicz, K.; Siemiarczuk, A.; Cowley, D. J.; Baumann, W. *Nouv. J. Chim.* **1979**, *3*, 443.

(9) Rettig, W. *Angew. Chem., Int. Ed. Eng.* **1986**, *25*, 971.

(10) Lippert, E.; Rettig, W.; Koutecky, V. B.; Heisel, F.; Miehe, J. A. *Adv. Chem. Phys.* **1987**, *68*, 1.

(11) Rettig, W. In *Topics in Current Chemistry*; Mattey, J., Ed.; Springer-Verlag: Berlin, 1994; p 253.

(12) Rettig, W. In *Fluorescence Spectroscopy, New Methods and Applications*; Wolbeis, O. S., Ed.; Springer-Verlag: Berlin, 1993; p 31.

(13) Rettig, W.; Baumann, W. In *Progress in Photochemistry*; *Photophysics*, Rabek, J. F., Ed.; CRC Press: Boca Raton, 1992; Vol. 6, p 79.

(14) Bhattacharyya, K.; Chowdhury, M. *Chem. Rev.* **1993**, *93*, 507.

(15) Zachariasse, K. A.; von der Haar, Th.; Hebecker, A.; Leinhos, U.; Kühnle, W. *Pure Appl. Chem.* **1993**, *65*, 1745.

(16) Von der Haar, Th.; Hebecker, A.; Il'ichev, Y. V.; Jiang, Y.-B.; Kühnle, W.; Zachariasse, K. A. *Recl. Trav. Chim. Pays-Bas* **1995**, *114*, 430.

(17) Zachariasse, K. A.; Groby, M.; von der Haar, Th.; Hebecker, A.; Il'ichev, Y. V.; Jiang, Y.-B.; Morawski, O.; Kühnle, W. *J. Photochem. Photobiol., A* **1996**, *102*, 59.

(18) Zachariasse, K. A.; Groby, M.; von der Haar, Th.; Hebecker, A.; Il'ichev, Y. V.; Morawski, O.; Rückert, I.; Kühnle, W. *J. Photochem. Photobiol., A* **1997**, *105*, 373.

(19) Jones, G. II; Jackson, W. R.; Choi, C. Y.; Bergmark, W. R. *J. Phys. Chem.* **1985**, *89*, 294.

(20) Gompbel, J. A. V.; Schuster, G. B. *J. Phys. Chem.* **1989**, *93*, 1292.

(21) Rechthaler, K.; Köhler, G. *Chem. Phys.* **1994**, *189*, 99.

(22) Soujanya, T.; Fessenden, R. W.; Samanta, A. *J. Phys. Chem.* **1996**, *100*, 3507.

(23) The application of the NBD derivatives has been recently reviewed: Chattopadhyay, A. *Chem. Phys. Lipids* **1990**, *53*, 1.

(24) Ghosh, P. B.; Whitehouse, M. W. *Biochem. J.* **1968**, *108*, 155.

(25) Fager, R. S.; Kutina, C. B.; Abrahamson, E. W. *Anal. Biochem.* **1973**, *53*, 290.

(26) Ferguson, S. J.; Lloyd, W. J.; Radda, G. K. *Biochem. J.* **1976**, *159*, 347.

(27) Longmuir, K. J.; Martin, O. C.; Pagano, R. E. *Chem. Phys. Lipids* **1985**, *36*, 197.

(28) Schmidt, N.; Gercken, G. *Chem. Phys. Lipids* **1985**, *38*, 309.

(29) Silvius, J. R.; Leventis, R.; Brown, P. M.; Zuckermann, M. *Biochemistry* **1987**, *26*, 4279.

(30) Chattopadhyay, A.; London, E. *Biochim. Biophys. Acta* **1988**, *938*, 24.

(31) Street, K. W., Jr.; Krause, S. A. *Anal. Lett.* **1986**, *19*, 735.

(32) Lytton, S. D.; Mester, B.; Libman, J.; Shanzer, A.; Cabantchik, Z. I. *Anal. Biochem.* **1992**, *205*, 326.

(33) Lytton, S. D.; Cabantchik, Z. I.; Libman, J.; Shanzer, A. *Mol. Pharmacol.* **1991**, *40*, 584.

(34) Frost, H.; Pacey, R. E. *Talanta* **1989**, *36*, 355.

(35) Ramachandram, B.; Samanta, A. *Chem. Phys. Lett.* **1998**, *290*, 9.

(36) Fery-Forgues, S.; Fayet, J. P.; Lopez, A. *J. Photochem. Photobiol., A* **1993**, *70*, 229.

(37) Perrin, D. D.; Armarego, W. L. F.; Perrin, D. R. *Purification of Laboratory Chemicals*; Pergamon Press: New York, 1980.

(38) Reichardt, C. *Solvents and Solvent Effects in Organic Chemistry*; VCH: Weinheim, 1988.

(39) Crosby, G. A.; Demas, J. N. *J. Phys. Chem.* **1971**, *75*, 1009.

(40) Bevington, P. R. *Data Reduction and Error Analysis for the Physical Sciences*; McGraw-Hill: New York, 1969.

(41) Dewar, M. J. S.; Zoebisch, E. G.; Healy, E. F.; Stewart, J. J. P. *J. Am. Chem. Soc.* **1985**, *107*, 3902.

(42) Dewar, M. J. S.; Dieter, K. M. *J. Am. Chem. Soc.* **1986**, *108*, 8075.

(43) Thomsen, C. L.; Thøgersen, J.; Keiding, S. R. *J. Phys. Chem. A* **1998**, *102*, 1062.

(44) Wortmann, R.; Krämer, P.; Glania, C.; Lebus, S.; Detzer, N. *Chem. Phys.* **1993**, *173*, 99.

(45) Schuddeboom, W.; Warman, J. M.; Biemans, H. A. M.; Mejler, E. W. *J. Phys. Chem.* **1996**, *100*, 12369.

(46) Woodford, J. N.; Pauley, M. A.; Wang, C. H. *J. Phys. Chem. A* **1997**, *101*, 1989.

(47) Mohanalingam, K.; Hamaguchi, H. *Chem. Lett.* **1997**, 157.

(48) Mohanalingam, K.; Hamaguchi, H. *Chem. Lett.* **1997**, 537.

(49) Khalil, O. S.; Seliskar, C. J.; McGlynn, S. P. *J. Chem. Phys.* **1973**, *58*, 1607.

(50) Lippert, V. E. *Z. Elektrochem.* **1957**, *61*, 962.

(51) Mataga, N.; Kaifu, Y.; Koizumi, M. *Bull. Chem. Soc. Jpn.* **1956**, *29*, 465.

(52) Mataga, N. *Bull. Chem. Soc. Jpn.* **1963**, *36*, 654.

(53) Ravi, M.; Samanta, A.; Radhakrishnan, T. P. *J. Phys. Chem.* **1994**, *98*, 9133.

(54) Cox, G. S.; Hauptman, P. J.; Turro, N. *J. Photochem. Photobiol.* **1984**, *39*, 597.

(55) Nagarajan, V.; Brearly, A. M.; Kang, T.; Barbara, P. F. *J. Chem. Phys.* **1987**, *86*, 3183.

(56) Mukherjee, S.; Chattopadhyay, A.; Samanta, A.; Soujanya, T. *J. Phys. Chem.* **1994**, *98*, 2809.

(57) Ōki, M. *Applications of Dynamic NMR Spectroscopy to Organic Chemistry*; VCH Publishers: Deerfield Beach, 1985.

(58) The results of X-ray crystallographic measurements are to be published elsewhere.

(59) This statement is based on the fact that the three bond angles around the amino nitrogen in 5NBD, as measured by X-ray crystallography, are 110.9°, 123.3°, and 125.8°.

(60) Lunazzi, L.; Macciantelli, D.; Grossi, L. *Tetrahedron* **1983**, *39*, 305.